Useful Model Systems for the Study of $S_{RN}1$ Chemistry in the Synthesis of Poly(arylene ether ketone)s

Katerina E. Dukes, Malcolm D. E. Forbes,* Antony S. Jeevarajan,† Anna M. Belu, Joseph M. DeSimone,* Richard W. Linton,* and Valerie V. Sheares

Venable and Kenan Laboratories, CB #3290, Department of Chemistry, University of North Carolina, Chapel Hill, North Carolina 27599-3290

Received September 13, 1995; Revised Manuscript Received January 29, 1996[⊗]

ABSTRACT: Factors contributing to the occurrence of the $S_{RN}1$ reaction during the synthesis of poly(arylene ether ketone)s are studied using a variety of analytical techniques. Product analysis of polymerization reactions and magnetic resonance studies on photochemical model systems were performed. The polymerization of 4,4′-dichlorobenzophenone with 4,4′-isopropylidenediphenol under basic conditions was run in four amide solvents: 1,3-dimethyl-3,4,5,6-tetrahydro-2(1*H*)-pyrimidinone (DMPU), 1-methyl-2-pyrrolidinone (NMP), 1,1,3,3-tetramethylurea (TMU) and *N*,*N*′-dimethylacetamide (DMAc). Molecular weights of the products followed the order M_n(DMAc) > M_n(NMP) > M_n(TMU) > M_n(DMPU). Simulations of time-resolved electron paramagnetic resonance (TREPR) spectra were used to identify the radicals produced by photoinduced hydrogen atom abstraction in each of the four solvents. Transient optical absorption was used to quantify the yield of radicals produced by reaction of triplet benzophenone-d_{10} with each solvent. Time-of-flight secondary ion mass spectrometry of the resulting oligomers showed evidence for hydrogen-terminated chain ends. Solvated electrons were observed from the photoionization of phenolates using TREPR. The relevance of this to single electron transfer events in these solvents, or with certain aryl halide monomers for polymer synthesis, is discussed.

Introduction

Poly(arylene ether)s are an important class of high-performance plastics, and mechanistic issues in the synthesis of these polymers continue to draw considerable attention. The widely accepted mechanism is aromatic nucleophilic substitution[1] (S_NAr), where a bis(aryl halide), activated by either a carbonyl or sulfone group, is condensed with a bisphenolate via an intermediate Meisenheimer complex as shown in Scheme 1. It is generally known that bis(aryl fluorides) with a carbonyl activating group result in high molecular weight polymers, whereas when the analogous bis(aryl chloride)s are used, lower molecular weight polymers are often obtained. Since longer reaction times with chlorine-containing monomers do not improve this general result, the issue is not the greater reactivity of aryl fluorides over aryl chlorides in S_NAr reactions. As shown by Percec et al.[2] and others[3], several other factors, in addition to the choice of aryl halide, may influence the achievement of high molecular weight with keto-activated monomers. This includes choice of bisphenolate, choice of solvent, and polymerization reaction conditions. Side reactions that limit polymer growth have been suggested, most notably the involvement of a radical mechanism of nucleophilic substitution known as the $S_{RN}1$ mechanism.[4]

For certain poly(arylene ether) syntheses involving aryl chloride monomer, Percec and co-workers[2d] have proposed a competition between S_NAr and single electron transfer (SET) reactions, the latter of which initiates the $S_{RN}1$ chemistry. Such a reaction sequence, which competes with the formation of polymer product, is depicted in Scheme 2. A possible termination step of the radical pathway is hydrogen atom abstraction from a suitable donor, e.g., the solvent. The presence of such a step accounts for cases where only oligomeric products are formed due to the presence of unreactive (hydrogen-terminated) end groups. Mohanty also supported the idea that an $S_{RN}1$ side reaction may limit the molecular weight and obtained favorable polymerization results from chlorine-containing monomer systems using a radical scavenger.[3a]

The issues of choice of aryl halide and phenol monomer for poly(arylene ether ketone) synthesis have been discussed in detail in papers by Percec and co-workers.[2a,d] From these studies, we have selected model systems to target specific reactions in the proposed mechanism, namely, those involving phenolate as an electron donor, aryl halide as an electron acceptor, and solvent as a hydrogen atom donor. Using the less active (chlorinated) monomers, we focus initially on the *effects of solvent choice* for the specific polymerization reaction outlined in Scheme 3. The solvents under investigation, whose structures are shown in Table 1, were 1,3-dimethyl-3,4,5,6-tetrahydro-2(1*H*)-pyrimidinone (DMPU), 1-methyl-2-pyrrolidinone (NMP), 1,1,3,3-tetramethylurea (TMU), and *N*,*N*′-dimethylacetamide (DMAc). A fundamental understanding of the partitioning of reactants between these two pathways (S_NAr and $S_{RN}1$) will lead to more predictability of the level of success of these polymerization reactions. The motivation for the present interdisciplinary study was to find small molecule model systems and new analytical techniques with which to investigate the $S_{RN}1$ pathway.

Time-resolved electron paramagnetic resonance (TREPR) spectroscopy has recently been used to study the primary events in the photodegradation of several alkyl-CO copolymers.[5] This technique provides the ability to detect free-radical intermediates with high sensitivity and fast time resolution. It has a significant advantage over steady-state EPR methods in that it detects the radicals on the submicrosecond time scale after their production by a pulse of light, and this is usually before any rearrangements can occur. Here we

* Authors to whom correspondence may be addressed.
† Current address: University of Alabama, Department of Chemistry, Tuscaloosa, AL 35484-0336.
⊗ Abstract published in *Advance ACS Abstracts,* March 15, 1996.

0024-9297/96/2229-3081$12.00/0

Scheme 1

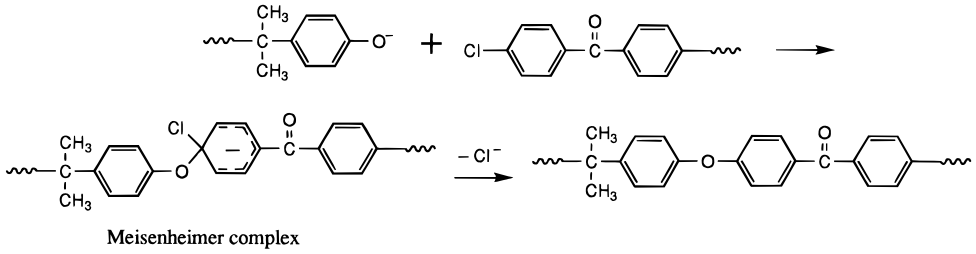

Scheme 2

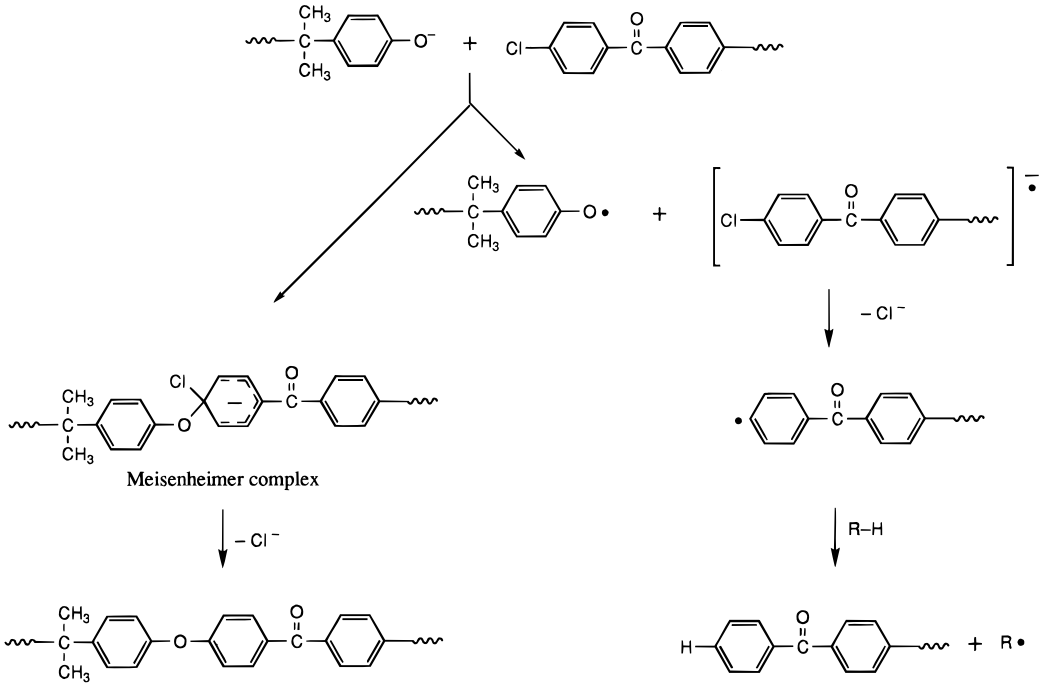

Scheme 3

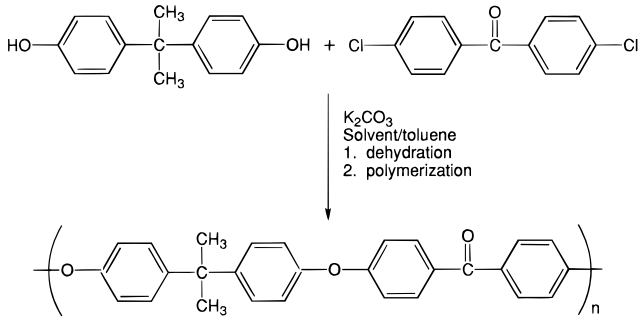

use TREPR to detect the most stable radicals formed in these amide solvents in the absence of S_NAr chemistry and fully characterize them by spectral simulation. Relative intensities of TREPR signals are used to give a qualitative estimate of the yield, and therefore stability, of each radical, and this is further quantified by transient optical absorption (TOA) spectroscopy in the case of solvent radicals.

In addition to gel permeation chromatography (GPC), polymers were characterized by time-of-flight secondary ion mass spectrometry (TOF-SIMS). The TOF-SIMS technique has an advantage[6] over traditional characterization methods in that it can determine absolute molecular weights and molecular weight distributions, and it can give quantitative information on end-group functionalization of polymers.

Additionally, we have investigated the photochemical reactions of phenols and phenoxides. Our preliminary

Table 1. Molecular Weights Obtained for Poly(arylene ether ketone)s Synthesized Using Scheme 3 in the Solvents Shown

solvent	structure	$\langle M_n \rangle^a$	MWD[a]
DMPU	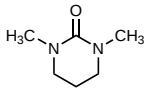	3000	1.99
NMP	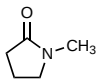	4000	2.09
TMU	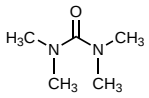	12000	2.08
DMAc	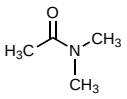	40000	2.08

[a] GPC results are vs poly(styrene) standards.

results show that it is possible to model an essential feature of the $S_{RN}1$ reaction mechanism: ejection of an electron from phenolate anion. Extension of the phenolate model system to include aryl halides as electron acceptors (or traps) shows that radical ion intermediates and substituted phenyl radicals can be observed in the TREPR experiment. The results of all our experiments strongly support the hypothesis that $S_{RN}1$-initiated chemistry is responsible for inhibiting polymer chain growth when conventional step-growth polymerization

is attempted in certain solvents with less active monomers.

Experimental Section

Polymer Synthesis. Typically, the polymer synthesis was conducted in a three-necked, 100-mL, round-bottom flask equipped with a mechanical stirrer, gas inlet, thermometer, Dean−Stark trap, and condenser. The flask was charged with 4,4′-dichlorobenzophenone (0.0159 mol) and 4,4′-isopropylidenediphenol (0.0159 mol) in 30 mL of DMAc via syringe. To this solution was added an excess of potassium carbonate (0.0478 mol). The salt was washed into the flask using 8 mL of DMAc; then ∼15 mL of toluene was added. This mixture was heated to reflux at an optimum temperature of 140 °C. Water generated during phenoxide formation was removed over a 6-h period. The reaction temperature was then increased to 170 °C for another 8 h. Completion of the polymerization was estimated by the increase in the viscosity. The polymer was coagulated in a 10-fold excess of a 50:50 methanol/water solution, then filtered, dried, and reprecipitated from chloroform into methanol.

Gel Permeation Chromatography. The apparent molar masses and molar mass distributions were analyzed by GPC using polystyrene standards with tetrahydrofuran as the mobile phase. The instrument was a Waters 1500-CV GPC equipped with Ultra Styragel columns with porosities of 100, 500, 10^3, 10^4, and 10^5 Å.

Time-of-Flight Secondary Ion Mass Spectrometry. The TOF-SIMS spectra were acquired using a TOF-II reflectron instrument developed and located at the University of Muenster.[7] Typical instrumental conditions during TOF-II spectrum acquisition were 1.2-pA primary Ar^+ current with a pulse width of 1 ns and a repetition rate of 150 μs. The primary ion beam struck a 0.25-mm^2 analysis area during a 200-s acquisition period. Thus, analysis conditions were maintained within the static regime with primary ion doses at $\sim 3 \times 10^{11}$ ions/cm^2. Postacceleration at 10 keV was employed. Samples were prepared by deposition of 1 μL of polymer solution in chloroform (1 mg/mL) onto 80 mm^2 of an etched silver substrate (monolayer preparation).

Model System Preparation for TREPR Studies. The synthesis was conducted in a 100-mL, three-necked round-bottom flask equipped with a thermometer, gas inlet, Dean−Stark trap, and condenser. The flask was charged with *tert*-butylphenol (0.0178 mol), potassium carbonate (2.7 g, 10% excess), 12 mL of a polar, aprotic solvent, and 8 mL of toluene. The reaction was heated while the toluene began to reflux (140 °C). Refluxing proceeded until all of the toluene was removed via the trap and dehydration was complete (10 h). The reaction mixture was then filtered, stored under nitrogen, and refrigerated until TREPR experiments were performed. For the aqueous solutions, 2.5 g of recrystallized 4,4′-isopropylidenediphenol (Bisphenol A) was added to a nitrogen-saturated 0.1 M NaOH solution. Equimolar amounts of *p*-bromo-, *p*-chloro-, and *p*-fluorobenzoic acid were added to respective Bisphenol A solutions for the quenching studies.

Time-Resolved EPR Spectroscopy. A JEOL USA Inc. X-band (JES-RE1X) spectrometer was used, which was equipped with a fast preamplifier (60-ns rise time). Solutions of our model compounds, as prepared above, were circulated through a 0.5-mm quartz flat cell placed in a Varian TE_{103} optical transmission EPR cavity. An excimer laser firing at a repetition rate of 60 Hz (308 nm, XeCl, 17-ns fwhm pulse width, ∼200 mJ/pulse) was used to excite the sample, typically consisting of a 0.01−0.1 M solution. The EPR signal at a given delay time (after the laser pulse) was collected directly from the microwave bridge, bypassing the usual phase-sensitive detection apparatus, and fed to a boxcar signal averager. The boxcar acts as a sample-and-hold device, operating in a two-gate mode, where one gate collects the EPR signal before the laser flash and the other collects the signal at a preset delay time after the laser flash. The signal was stored digitally as the difference between the two gates (light minus dark). Typical gate widths and delay time were 100 ns and 1 μs, respectively. The Q-band TREPR apparatus is that described in our earlier work,[8] except that the source and detector improvements described by Hyde et al.[9] have been implemented.

Scheme 4

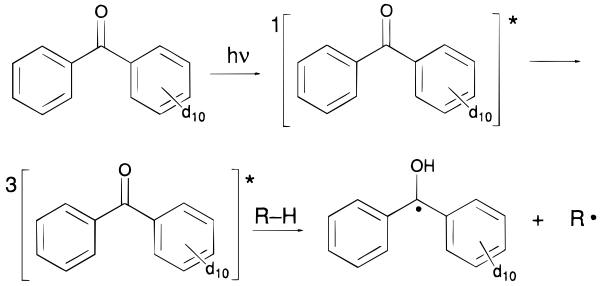

Transient Optical Absorption Spectroscopy. Transient absorption measurements were conducted using a Quanta Ray DCR Nd:YAG laser (355 nm) to irradiate the sample solutions. The excitation beam was synchronized with the monitoring beam of an Applied Photophysics laser kinetic spectrometer. This included a 250-W pulsed Xe arc probe source, a *f*/3.4 grating monochromator, and a five-stage PMT. The output was coupled to a LeCroy 9400 digital oscilloscope interfaced to an IBM-PC. Sample solutions consisted of benzophenone-d_{10} in distilled benzene and benzophenone-d_{10} in distilled benzene with each of the four amide solvents listed in Table 1 as quenchers. Five different concentrations of quencher were used for each individual analysis, using benzophenone-d_{10} to quencher ratios of 1:1, 1:2, 1:3, 1:4, and 1:5 equiv. Large quantities of quencher were avoided due to interfering absorbance of the amides at high concentrations. The solutions were deoxygenated by bubbling with dry nitrogen. Evolution of the signal from triplet benzophenone-d_{10} was monitored at 600 nm.[10] Absorbance vs time decay data fit well with single exponential decay kinetics.

Results and Discussion

The reaction investigated (Scheme 3) is the polymerization of 4,4′-dichlorobenzophenone (DCBP) with Bisphenol A. The solvents are suitable for classical substitution chemistry because of their dipolar, aprotic character.[11] They share similar physical properties, notably high dielectric constants ranging from 23.6 (for TMU) to 37.8 (for DMAc), and boiling points around 200 °C. Under similar conditions (temperature, concentration, reaction time) these monomers were polymerized in the four amide solvents. As shown in Table 1, the solvent significantly influences the final molecular weight. It is not likely that the minor polarity differences among these solvents will have a dramatic effect on the polymer-forming S_NAr reaction (which involves charged transition states), and it is even less likely that these polarity differences will have a significant impact on a series of neutral radical reactions. If the solvents participate as reagents in the reaction scheme as hydrogen atom donors, we would like to know the resulting solvent radical structures and relative thermodynamic stabilities, and whether or not there is a correlation of these properties with the molecular weights achieved in the polymerization reactions. We begin our discussion with magnetic resonance results used to identify the radicals and to see how easily they may be formed in the absence of classical substitution chemistry.

The well-established photochemistry of benzophenone in hydrogen donor solvents is detailed in Scheme 4. The first excited singlet-state intersystem crosses within 10 ps to the first excited triplet state, from which hydrogen atom abstraction from solvent molecules usually occurs with a time constant of several hundred nanoseconds.[12]

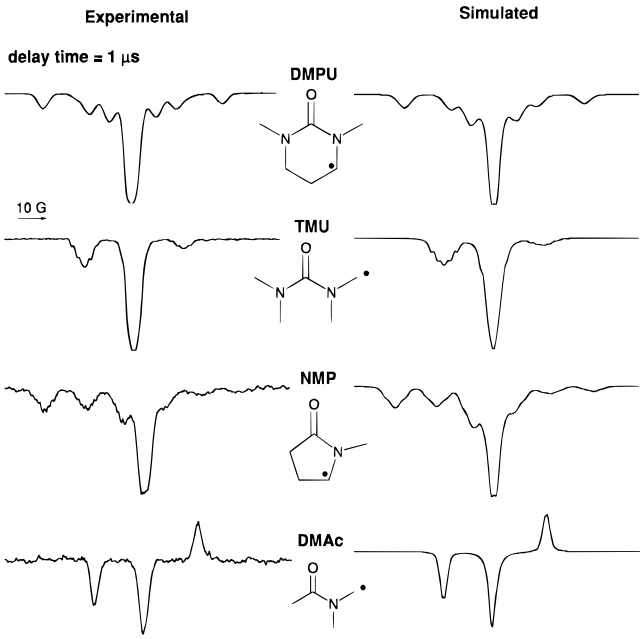

Figure 1. Left: Experimental TREPR spectra of 0.01 M solutions of benzophenone-d_{10} in the indicated solvents. Right: Simulations of the TREPR spectra shown on the left. Magnetic parameters of the solvent radicals are listed in Table 2. A hyperfine coupling constant of 2.0 G for the hydroxyl hydrogen was used for the diphenylhydroxymethyl radical.

Amide solutions of benzophenone-d_{10} (0.01 M) were flash photolyzed in the EPR spectrometer. Photochemical creation of radicals was preferred as it allowed pulsed production and time-resolved detection. This allows the observation of the initial radicals produced upon hydrogen atom abstraction and not radicals that are the product of a rearrangement.

The experimental TREPR spectra, which were each collected at delay times of 1 μs after the laser flash, are shown on the left side of Figure 1 for the four solvents of interest. In all four spectra the central transition is due to the benzophenone ketyl radical (hydroxydiphenylmethyl), while all other transitions are due to radicals from the solvent. Deuteration of the phenyl rings of the benzophenone lowers the ring hyperfine coupling constants by a factor of 6.4, reducing the width of the central signal substantially. This gives spectra with better resolution of signals from other radicals. The spectra are unusual in appearance due to the presence of chemically induced dynamic electron spin polarization (CIDEP),[13] which causes non-Boltzmann populations of spin states to exist at the time of observation. Note that the EPR spectra in this and in all subsequent figures are displayed in direct detection and not in the first-derivative mode typical of steady-state EPR. The transitions below the baseline in Figure 1 show emission, while those above the baseline exhibit enhanced absorption. There are actually two spin polarization mechanisms at work here. Both mechanisms are well established experimentally and theoretically, and the reader is referred to any of several monographs for details.[14] The radical pair mechanism (RPM), which arises due to nuclear spin selective singlet−triplet mixing of radical pairs, gives a polarization pattern that is emissive for low-field transitions and absorptive for the high-field ones. Superimposed on this pattern is a net emission from the triplet mechanism (TM), which arises due to net polarization produced in the $S_1 \rightarrow T_1$ intersystem crossing process in the parent molecular ketone. Note that the magnitude of the TM polarization, quantified by the amount of net emission in the high-field transitions, is different in each solvent. The TM magnitude depends on the degree of motional averaging of the zero-field splitting in the ketone triplet state and, therefore, on the viscosity of the solution. Indeed, the simulations, to be discussed below, show that the ratio of TM to RPM polarization is directly proportional to the viscosity of each of the four solvents.

Table 2. Magnetic Parameters Used in Simulations of Spectra in Figure 2

radical structure	hyperfine coupling constants (G)	line width (G)
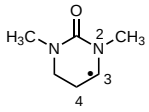	H4 = 22.5 H3 = 15.8 N2 < 1	3.0
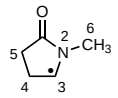	H4 = 26.5 H3 = 14.0 H5 = 3.0 H6 < 1 N2 = 1.0	1.8
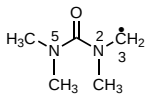	H3 = 16.6 N2 = 2.3 N5 = 2.0	1.8
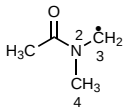	H3 = 17.2 H4 = 1.0 N2 < 1	1.1

Simulations of the TREPR data, shown on the right side of Figure 1, allowed unequivocal characterization of the most stable free radical formed by hydrogen atom abstraction from each solvent. In all four spectra only one solvent radical signal dominates the spectrum. This indicates that radical stability may be a key parameter dictating the abstraction reaction rate. Table 2 lists the values of hyperfine coupling constants obtained from the simulations of the four spectra. Simulation parameters for the hydroxydiphenylmethyl radical are taken from the literature.[15] For TMU and DMAc, it is only possible to obtain primary alkyl radicals. There are several possible secondary radicals that can be produced from DMPU and NMP. The ones we observe are those radicals which are stabilized by resonance forms that extend spin density onto the carbonyl group. Presumably, solvents from which a secondary carbon-centered radical could be produced would be the best hydrogen donors and therefore the most likely in an $S_{RN}1$ scheme to terminate a polymer chain (i.e., they represent a poor solvent choice for polymer syntheses involving radical pathways). This assumption seems valid since only oligomeric products were synthesized in DMPU and NMP. Thermodynamic stability is significant when one considers a radical reaction solely, but as we will discuss below, the kinetics of the process should be considered as well.

Comparison of overall TREPR intensities between the four solvents and relation of these intensities to radical yield and/or stability is problematic because of the spin polarization. Absolute polarization magnitudes are, at present, not measurable with our apparatus. This means that we cannot account quantitatively for the difference in overall radical concentrations for the four spectra in Figure 1. Qualitatively, it is easy to rationalize the strong signal for DMPU vs the weak signal for DMAc (here we are just estimating signal intensities based on signal-to-noise ratios and gain settings on the TREPR spectrometer). In DMPU there are 10 sites for

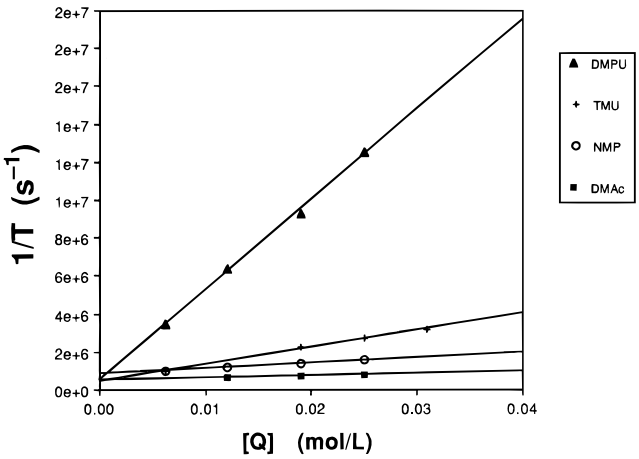

Figure 2. Stern−Volmer plots for the quenching of triplet benzophenone-d_{10} in benzene via bimolecular reaction with the solvents shown in Table 1.

hydrogen atom abstraction which can lead to a resonance-stabilized alkyl radical, centered on a carbon α to a nitrogen. However, only four of these lead to the more stable secondary alkyl radical shown to dominate the TREPR spectrum. In DMAc there are six abstraction sites, but all lead to less stable primary alkyl radicals. Since the transition state in the abstraction reaction has substantial radical character, a lower activation energy is expected for reactions leading to secondary radicals than those leading to primary ones. For this reason, the rate, and therefore the yield, of secondary radicals should be greater than primary radicals. However, frequency factors for the rate constant will depend on the number of available abstraction sites, which is different for each solvent. As such, it appears that the difference between DMPU and NMP is due to the greater number of sites available for abstraction in DMPU. The same argument holds for the intensity difference between TMU and DMAc. The most difficult comparison is between TMU and NMP, where it appears that the signal due to primary radicals from TMU is comparable or slightly stronger than that due to the secondary radicals from NMP. It should be noted that the viscosity of these two solvents is almost the same (1.3 vs 1.5 cP),[16] and so the magnitude of the triplet mechanism spin polarization should be similar in both cases. The 12 sites available for abstraction in TMU statistically outweigh the five sites available in NMP (only two of which lead to the secondary carbon-centered radical identified in the TREPR spectrum). Therefore, while the primary TMU radical may be less stable than secondary NMP radical, the greater frequency factor in the TMU case may account for a slightly greater intensity compared to the NMP case. Clearly there is a delicate balance between kinetic and thermodynamic effects on the TREPR intensities. Reasons for this become more apparent when the transient optical absorption data is considered.

The yield of radicals can be quantified by measuring the lifetime of the triplet benzophenone-d_{10} in benzene as a function of quencher (amide solvent) concentration, if we assume that the major decay pathway for the triplet is via abstraction of hydrogen from the quencher. Based on the very strong radical signal intensities measured by TREPR, this assumption seems valid for all four solvents. From our TOA data, shown in Figure 2, we were able to obtain the Stern−Volmer plots of triplet lifetime (T) vs amide concentration using benzene as a solvent. At each concentration, the rate of disappearance of the triplet follows the same trend as the TREPR data. Analysis of these plots by linear regression gave bimolecular rate constants, listed in Table 3, for the decay of the triplet following the order $k_{DMPU} > k_{TMU} > k_{NMP} > k_{DMAc}$. This is the same trend observed for the intensity differences for the TREPR data in Figure 1. We can now rationalize these intensity differences for a given delay time, notably in the TMU and NMP spectra, by taking into account the frequency factors for the rate constant as discussed above. Only the most thermodynamically stable radicals formed from each solvent are identified by simulation of their TREPR spectra, but the signal intensities are also governed by the kinetics of the abstraction process. Thus, we can rationalize a slightly higher intensity for TMU radical vs that of NMP radical based on the relative differences in rate constants (1×10^8 vs 3×10^7 M^{-1} s^{-1}), which take into account the number of available abstraction sites (12 vs 2).

Table 3. Bimolecular Rate Constants Measured for the Quenching of Triplet Benzophenone-d_{10}

quencher	k (M^{-1} s^{-1})
DMPU	5×10^8
TMU	1×10^8
NMP	3×10^7
DMAc	1×10^7

On the basis of this magnetic resonance and optical data, we can state that the more thermodynamically stable the radical formed from solvent, the more likely it becomes that a divergent pathway involving free radicals will produce hydrogen-terminated oligomers. It should be emphasized that this statement holds true for a radical pathway exclusively (which is the case in our TREPR experiments) and not when there is competition with a classical substitution pathway. Furthermore, this is not to say that the termination step drives the radical reaction sequence proposed in Scheme 2 in either the absence or the presence of competitive chemistry. For now, we conclude our analysis of the termination step by presenting the TOF-SIMS data, which provide strong evidence that hydrogen atom abstraction takes place during the synthesis in at least one of the four solvents.

A TOF-SIMS spectrum for the polymer synthesized in NMP is shown in Figure 3. The sensitivity of TOF-SIMS enables one to observe the signals corresponding to intact polymer chains at each degree of polymerization. Each set of peaks, separated by the mass of the polymer repeat unit (406 g/mol), corresponds to the mass of a single degree of polymerization, including the repeat unit, the silver cation (which aids in the ionization process), and either the hydrogen or the hydroxyl end group. The resolution of this technique is greater than 1 amu and allows one to see individual signals for each degree of polymerization which result from the various combinations of carbon and silver isotopes. The high-mass range of the TOF-SIMS spectrum (900−2500 Da) for the polymer synthesized in NMP is shown in Figure 3A. The most intense signals in the high-mass range result from the desorption of intact oligomer chains with a specific degree of polymerization (n). From the masses of the signals, three distinct oligomeric species are identified, where $n = 2-5$. The basic repeat unit of all oligomers is the same, but the oligomers are distinguished by the end-capping monomers (Figure 3B). The following can be summarized from from the combination of GPC and TOF-SIMS analysis. First, when dichlorobenzophenone and 4,4′-isopropylidenediphenol are

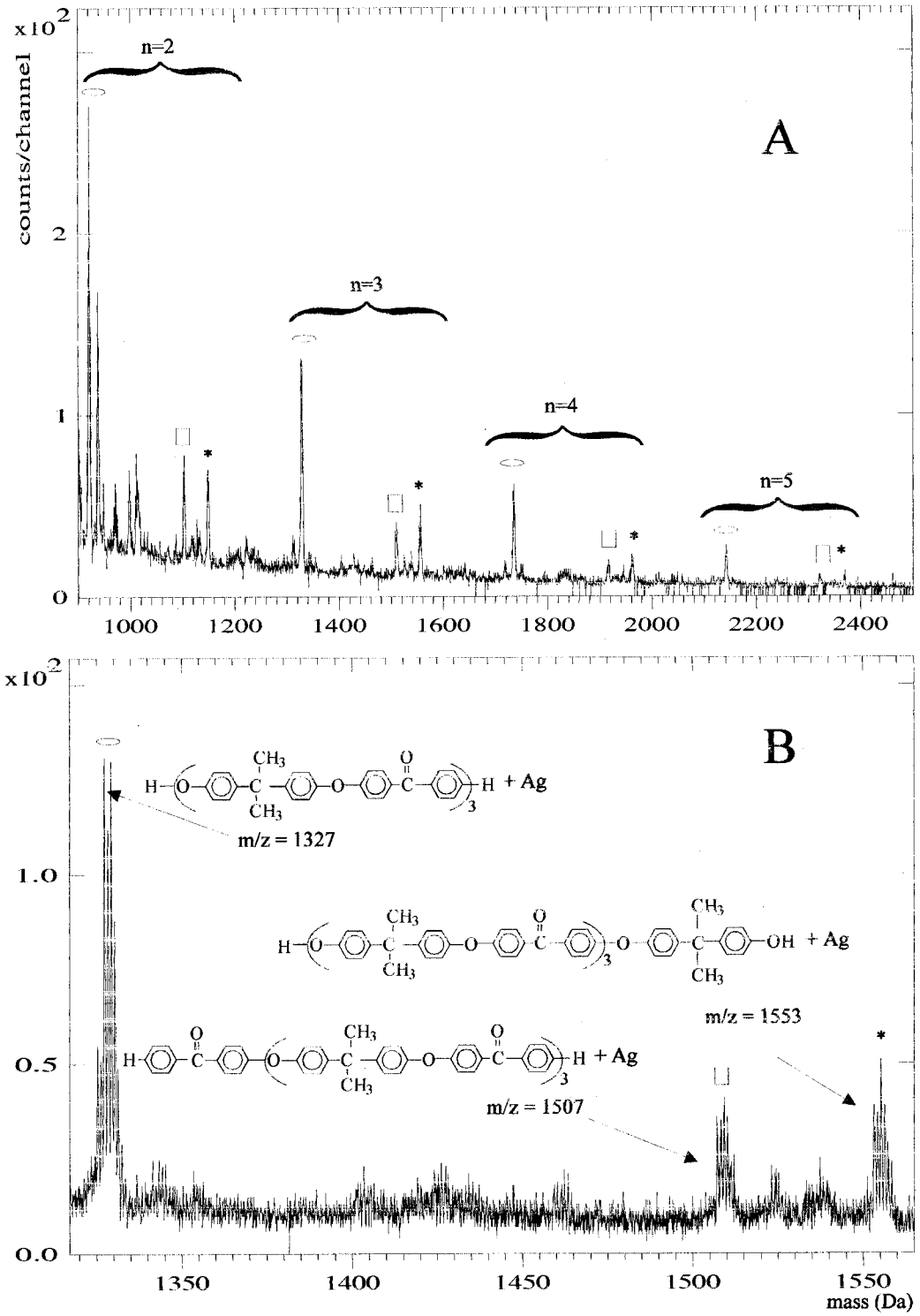

Figure 3. (A) TOF-SIMS spectrum showing the high molar mass range of the poly(arylene ether ketone) shown in Scheme 3, synthesized in NMP. (B) Expanded view of the mass range of the $n = 3$ oligomers from spectrum in (A).

polymerized in DMAc, high molecular weight (M_n greater than 40 000 and distributions of 2.01 by GPC) can be obtained in 8−12 h. Second, when the same polymerization is mediated by NMP, low molar masses (M_n 2000−4000 by GPC) are obtained and the chlorine atom end groups of the oligomeric species have been replaced by hydrogens, indicative of an alternate reaction pathway.

A quantitative comparison of TOF-SIMS signal intensities was made among the different oligomeric species. Since the oligomers have a similar molar mass and chemical composition, the sputter yield, ionization, and detection probabilities are thought to be constant for all species. Fragmentation of the oligomers, however, is evident from signals arising 2 Da lower than the intact oligomer signals. Due to the isotopic distribution of peaks within a signal, the fragment signal must be deconvoluted from the intact oligomer signal for accurate quantitative analysis. After deconvolution, the areas of the intact oligomer signals can be compared, and these are listed in Table 4 for the TOF-SIMS spectrum shown in Figure 3A. Indeed, the ratio of relative quantities of oligomers (for each degree of polymerization $n = 2-5$) is in good agreement with the

Table 4. Relative TOF-SIMS Signal Intensities (Figure 3A) of Intact Oligomers at Each Degree of Polymerization

	end-capping monomer	theor	$n = 2$	$n = 3$	$n = 4$	$n = 5$
oval	DCBP/Bisphenol A	0.50	0.52	0.51	0.55	0.56
□	DCBP/DCBP	0.25	0.26	0.23	0.22	0.21
*	Bisphenol A/Bisphenol A	0.25	0.22	0.26	0.23	0.23

Scheme 5

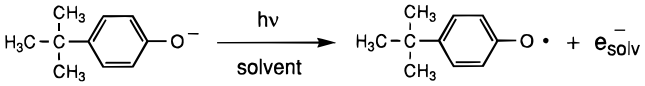

statistical values expected if all the Cl end groups have been displaced by hydrogens: 50% hydrogen/hydroxyl, 25% hydroxyl/hydroxyl, and 25% hydrogen/hydrogen end groups.

These mass spectral data are in agreement with ^1H NMR data from our laboratory and from that of Percec,[2a] where benzophenone end groups were only detectable in the low molecular weight species and not in longer polymer chains. The TOF-SIMS experiment is only feasible using the lowest of the molecular weights, i.e., the oligomeric species formed in DMPU and NMP. It is possible that another mechanism may account for some of the oligomeric product synthesized in NMP as it has been documented that NMP degrades at the times and temperatures utilized for the polymerization.[17] It should also be noted that reductive dehalogenation using NMP as solvent (one reaction step prior to the termination step in Scheme 2) can take place in the absence of phenolate.[2c,d] From the present study, however, the NMP data appear to best support the proposed side reaction out of these four solvents. Further study of these reactions in NMP using TOF-SIMS is presently underway in our laboratories.

In addition to the issues discussed above, it is apparent that an understanding of the factors that initiate the proposed radical chemistry and an understanding of the factors that may govern the subsequent dehalogenation step prior to termination would be of practical significance. To investigate single electron-transfer events and the promotion of the $S_{RN}1$ reaction under the polymerization conditions, the photoionization of a phenoxide was attempted in the TREPR experiment for each solvent. Photolysis of phenoxides leads to phenoxyl radicals and solvated electrons, e^-_{solv},[18] as shown in Scheme 5. The 4-*tert*-butylphenol molecule was chosen as a model compound for 4,4′-isopropylidenediphenol. The impetus for this set of experiments was to identify the phenoxyl radical, one of the intermediates in the proposed $S_{RN}1$ chemistry, and to see whether other radical species, e.g., from the solvent, could be observed. Experimental TREPR spectra of this model system in each of the various solvents are shown in Figure 4. Clearly, in all four solvents, the spectra display a similar polarization pattern (emission/absorption) and similar hyperfine splitting. However, solvent radicals, as identified from the simulations in Figure 1, are not observed in Figure 4. This means that amide solvent radicals are not formed from abstraction of hydrogen by phenoxyl radical, a result in line with the known high stability of phenoxyl due to resonance into the phenyl ring.[19] This result is also in agreement with the proposed radical sequence in which termination involves a phenyl, not phenoxyl, moiety.

Simulation of the spectra in Figure 4 confirmed the presence of the phenoxyl radical/e^-_{solv} pair in each

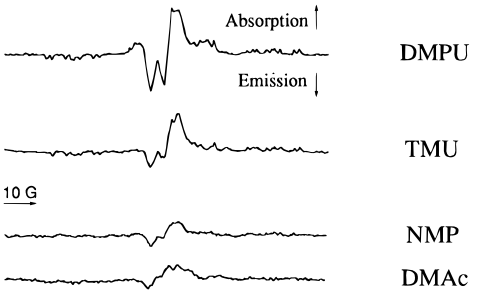

Figure 4. Experimental TREPR spectra for the photoionization of 0.1 M 4-*tert*-butylphenol in the solvents listed on the right.

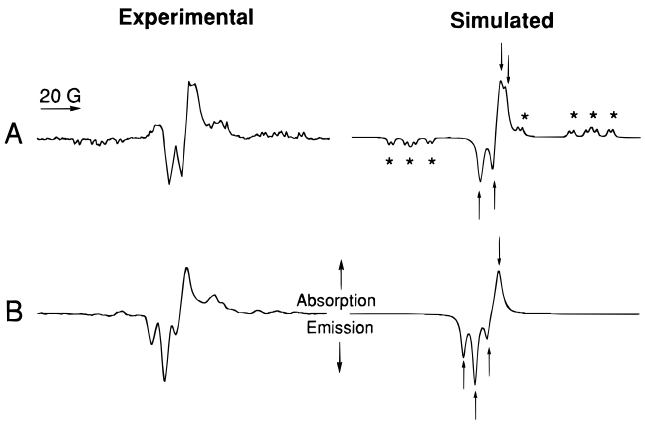

Figure 5. Experimental and simulated TREPR spectra of the *tert*-butyl phenoxide system in DMPU solvent at (A) X-band and (B) Q-band frequencies. Arrows in (A) represent overlapping signals for the phenoxyl radical/solvated electron pair. Asterisks in (A) denote a cyclohexadienyl-type radical formed from the substituted phenol. Arrows in (B) denote phenoxyl radical in emission and solvated electron in absorption. Delay times are 1.0 and 0.1 μs, for X- and Q-band frequencies, respectively.

solvent. The intensity differences, however, suggest that the yield of radicals is different in each case. This is an interesting point to consider from the perspective of $S_{RN}1$-initiating reactions. Although we have photochemically generated the phenoxyl radical and electron in our experiments, there should be a similar correlation of the yields of these species formed in an analogous thermal reaction. Attempts to detect radicals thermally in the same model system and in the actual polymerization system by steady-state EPR were unsuccessful.

Figure 5 shows the experimental and simulated TREPR spectra for the model system in Scheme 5 run in DMPU solvent. The bottom was obtained using a Q-band TREPR (35.5 GHz) apparatus, which gives us better resolution of the phenoxyl radical signal (low-field lines) and the e^-_{solv} signal (high-field line). The photophysics of phenoxides and phenols depends on the medium[20] and excitation wavelength.[21] Moreover, there continues to be debate regarding the nature of the excited-state precursor of photoionized phenol derivatives. There is evidence, for example, that in alkaline solution the singlet state of the phenolate ejects an electron, while in neutral solution the triplet state of the phenol (conjugate acid) is reponsible for the same photochemical result.[20a] But there is other evidence for photoejection from the triplet excited state for both phenol and phenolate derivatives.[20b,c] The redox potentials of phenols are also a function of acid/base equilibria and are typically 0.5 V higher for a phenol in neutral solution vs the corresponding phenol at high pH.[22] Clearly then, the extent of photochemistry in-

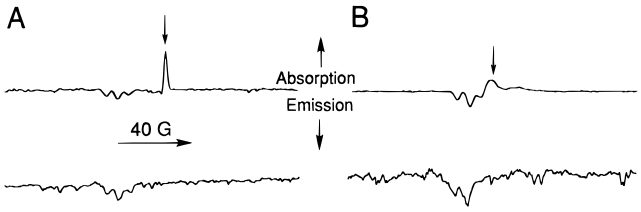

Figure 6. Experimental Q-band TREPR spectra of substituted phenolates in (A) basic aqueous solution and (B) DMPU solvent. (A) 4-*tert*-butylphenoxyl radical (emissive) and hydrated electron (absorptive) in N_2-saturated solution (top spectrum) and in N_2O-saturated solution (bottom spectrum). (B) Phenoxyl radical from Bisphenol A (emissive) and solvated electron (absorptive) in N_2-saturated solution (top) and N_2O-saturated solution (bottom). Arrows denote e^-_{solv} in the upper spectra. Time delay is 0.1 μs for all spectra.

volving the phenol derivative as opposed to its dissociated form needs to be considered in interpreting the TREPR results. Since our model compound is prepared under the same polymerization conditions as those to create the dianion (Scheme 3), we assume that most of the photochemistry arises from the phenolate. As a control, all of our experiments involving phenols were first run in neutral solution. We can be convinced that the photochemistry is taking place from phenoxide when the same system in neutral solution shows no signal. Except for the case of DMPU solvent, no TREPR signal was observed in the absence of added base.

There are two additional radical signals observed in these spectra. One is the weak signal with many hyperfine lines on the periphery of the top spectra in Figure 4. It is most clearly seen with DMPU as solvent and indicated by asterisks in Figure 5A. This was identified by spectral simulation as a substituted cyclohexadienyl radical[23] due to net hydrogen transfer to the phenyl ring. Since solvent radicals were not detected in this spectrum, the hydrogen atom donor in this case is uncertain. Although the concentration of phenol is expected to be low, the hydroxyl group of phenol may be the hydrogen source. There is a likely pK_a shift upon photoexcitation of phenol.[24] A lower pK_a for the excited-state phenol would deem it a suitable hydrogen atom donor. Furthermore, pK_a differences between ground and excited states of phenol will help address the controversies surrounding the photoionizing state of substituted phenols,[25] but this is a topic beyond the scope of this paper. The other extra signal in Figure 5 is at present unidentifiable. It appears as an absorptive triplet, which overlaps with the phenoxyl signal and decays quickly compared to the other signals. It may be a radical anion formed by the trapping of e^-_{solv} by a neutral species, which would carry a net absorptive polarization transferred from the electron.

Figure 6A shows the Q-band spectra obtained upon photolysis of *tert*-butyl phenol in aqueous NaOH solution (pH 12). In the top spectrum of Figure 6A, the phenoxyl radical appears as three lines in emission while the hydrated electron appears as a single absorptive peak, just as in Figures 4 and 5, only now the e^-_{solv} signal is better separated from the phenoxyl radical. This is indicative of a greater *g*-factor difference in aqueous solution vs the amide solution. The lower spectrum in Figure 6A shows the spectrum obtained from the same solution after it has been saturated with nitrous oxide, an efficient electron scavenger.[20b] The signal assigned to e^-_{solv} disappeared, as expected. The same TREPR experiment was performed using the monomer Bisphenol A. The top of Figure 6B shows the

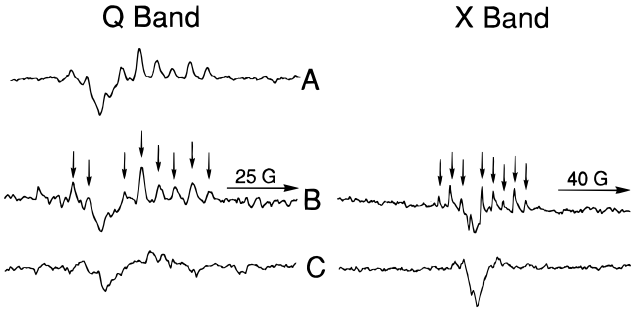

Figure 7. Experimental Q-band and X-band TREPR spectra of Bisphenol A in basic solution with halobenzoic acids added as radical scavengers (see Scheme 6): (A) 4-bromobenzoic acid, (B) 4-chlorobenzoic acid, and (C) 4-fluorobenzoic acid. Arrows denote signal from carboxy-substituted phenyl radical. Delay times are 0.1 and 0.5 μs for Q- and X-band frequencies, respectively.

Scheme 6

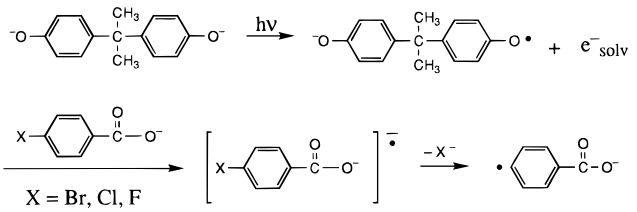

spectrum of phenoxyl radical (emissive) and solvated electron (absorptive) from Bisphenol A monomer in DMPU solution. This spectrum is nearly identical to that in Figure 5B (from *tert*-butyl phenol), and we can further confirm the assignment of the solvated electron by scavenging with N_2O, as shown in the lower spectrum of Figure 6B. Further work to understand the photophysics of these systems in aqueous and nonaqueous environments, particularly with regard to spin state, is ongoing. It is noteworthy that the phenoxyl/e^-_{solv} radical pair is observable in all four solvents, which supports the possibility of a single electron-transfer reaction initating an alternative pathway to the polymerization reaction.

Extension of the time-resolved experiment to the conditions of polymerization using Bisphenol A and DCBP monomers was not very informative because the photochemistry at 308 nm is overwhelmed by the benzophenone moiety and not the phenoxide. However, we have performed a set of experiments using aryl halides as solvated electron traps. Benzoic acid derivatives were used to model carbonyl-activated aryl halides used in actual polymerizations. These experiments were run in basic aqueous solution. The photochemistry of the phenolate, depicted in Scheme 6, will dominate at the wavelength used in the experiment. The dianion of Bisphenol A was the electron source and a series of halo derivatives of benzoic acid were the electron acceptors. Photoejection of an electron by the phenolate leads to formation of the radical anion of the benzoate, which quickly loses the halide ion to generate a substituted phenyl radical. These phenyl radicals were observable by TREPR, depending on the halide substituent. The left side of Figure 7 shows the Q-band results using Br-, Cl-, and F-substituted benzoates. In the case of bromo- and chlorobenzoate acceptors, *para*-subtituted phenyl radicals show nine absorptive lines of the respective spectra, a few of which are obscured by the emissive lines characteristic of the phenoxyl radical. The right side of Figure 7 shows the corresponding X-band result, which for the chlorinated

benzoate helps in identifying these signals. In the case of the fluorinated benzoate, no phenyl radical was observed at these and later delay times (>1 μs). The absence of the e^-_{solv} suggests that formation of the aryl fluoride radical anion has occurred. However, the poor signal-to-noise ratio makes this spectrum difficult to assign. The data set in Figure 7 clearly indicate that the loss of halide initiated by SET is possible and the ensuing phenyl and phenoxyl radicals are detectable in our experiment. Furthermore, this chemistry can be carried out on molecules of an electronic structure very similar to those used in the polymerization reaction.

Summary

The polymerization of DCBP and Bisphenol A in several amide solvents has been used to investigate the mechanism of poly(arylene ether ketone) synthesis. Model systems for several steps in the synthesis were developed and their utility was demonstrated. Identification of the most stable radical formed from each of four amide solvents was successful. Radical stabilities were consistent with product analyses in that poor solvent choices were those which formed secondary, resonance-stabilized, carbon-centered radicals. Relative rates of hydrogen atom abstraction from each solvent follow the order $k_{DMPU} > k_{TMU} > k_{NMP} > k_{DMAc}$. The TOF-SIMS data offer mass spectral evidence for hydrogen end groups under reaction conditions that result in oligomeric products. We were able to quantify the distribution of end groups and determine that no chlorine chain ends are present for the polymerization of DCBP and Bisphenol A in NMP solvent. These results add strong support to the conclusions of Percec et al. from their NMR analyses of unreactive polymer chain ends. The TREPR spectra of phenoxyl radical/e^-_{solv} displayed an intensity dependence that also correlates with the synthetic results, showing that the extent of radical side reactions depends on solvent choice. The identification of radical ions and phenyl radicals produced from aryl halides also demonstrates that the choice of halide as an effective leaving group is important in the partitioning of a radical pathway vs a classical substitution reaction. The model systems and physical methods described here will be useful for further investigation of the SET process in the $S_{RN}1$ reaction and other mechanisms.

Acknowledgment. This work was supported by the National Science Foundation through Grant CHE-9522007 (M.D.E.F.); by the NSF through a Presidential Faculty Fellowship (J.M.D., 1993−1997), the Thiophene-based Materials Consortium at UNC sponsored by the Office of Naval Research, and Hoechst-Celanese Corp.; and by Monsanto and the North Carolina Board of Science and Technology (R.W.L.).

References and Notes

(1) Rose, J. B. In *Recent Advances in Mechanistic and Synthetic Aspects of Polymerization*; Fontanille, M., Guyot, A., Eds.; D. Reidel Publishing Co.: Boston 1987; p 207.

(2) (a) Percec, V.; Clough, R. S.; Rinaldi, P. L.; Litman, V. E. *Macromolecules* **1991**, *24*, 5889. (b) Percec, V.; Wang, J. H.; Clough, R. S. *Makromol. Chem., Macromol. Symp.* **1992**, *54/55*, 275. (c) Percec, V.; Clough, R. S.; Grigoras, M.; Rinaldi, P. L.; Litman, V. E. *Macromolecules* **1993**, *26*, 3650. (d) Percec, V.; Clough, R. S.; Rinaldi, P. L.; Litman, V. E. *Macromolecules* **1994**, *27*, 1535.

(3) (a) Mani, R. S.; Zimmerman, B.; Bhatnagar, A.; Mohanty, D. K. *Polymer* **1993**, *34*(1), 171. (b) Sheares, V. V.; Belu, A. M.; Dukes, K. E.; Linton, R. W.; Forbes, M. D. E.; DeSimone, J. M. *Polym. Mater. Sci. Eng.* **1993** *69* (2), 247 (Polym. Prepr.).

(4) Bunnett, J. F. *Acc. Chem. Res.* **1978**, *11*, 413.

(5) Forbes, M. D. E.; Barborak, J. C.; Dukes, K. E.; Ruberu, S. R. *Macromolecules* **1994**, *27*, 1020.

(6) (a) Hunt, M. O., Jr.; Belu, A. M.; Linton, R. W.; DeSimone, J. M. *Macromolecules* **1993**, *26*, 4854. (b) Belu, A. M.; Hunt, M. O., Jr.; DeSimone, J. M.; Linton, R. W. *Macromolecules* **1994**, *27*, 1905.

(7) Niehuis, E.; Heller, T.; Feld, H., Benninghoven, A. *J. Vac. Sci. Technol. A* **1987**, *5* (4), 1243.

(8) (a) Forbes, M. D. E. *J. Phys. Chem.* **1992**, *96*, 7836. (b) Forbes, M. D. E. *Rev. Sci. Instrum.* **1993**, *64*, 397.

(9) Hyde, J. S.; Newton, M. E.; Strangeway, R. A.; Camenisch, T. G.; Froncisz, W. *Rev. Sci. Instrum.* **1991**, *62*, 2969.

(10) Scaiano, J. C.; Abuin, E. B.; Stewart, L. C. *J. Am. Chem. Soc.* **1982**, *104*, 5673.

(11) (a) Lüttringhaus, A.; Dirksen, H. W. *Angew. Chem., Int. Ed. Engl.* **1964**, *3*, 260. (b) Barker, B. J.; Rosenfarb, J.; Caruso, J. A. *Angew. Chem., Int. Ed. Engl.* **1979**, *18*, 503. (c) Mukhopadhyay, T.; Seebach, D. *Helv. Chim. Acta* **1982**, *65* (1), 385.

(12) (a) Scaiano, J. C.; Selwyn, J. C. *Can. J. Chem.* **1981**, *59*, 2368. (b) Scaiano, J. C.; Abuin, E. B.; Stewart, L. C. *J. Am. Chem. Soc.* **1982**, *104*, 5673.

(13) Molin, Yu. N., Ed. *Spin Polarization and Magneic Effects in Radical Reactions*; Elsevier: New York, 1984.

(14) (a) Trifunac, A. D.; Lawler, R. G.; Bartels, D. M.; Thurnauer, M. C. *Prog. React. Kinet.* **1986**, *14*, 43. (b) McLauchlan, K. A. In *Advanced EPR: Applications in Biology and Biochemistry*; Hoff, A. J., Ed.; Elsevier: New York, 1990; pp 345−369. (c) *Spin Polarization and Magnetic Effects in Radical Reactions*; Molin, Y., Ed.; Elsevier: New York, 1984; pp 224−242.

(15) Landolt-Bornstein, *Magnetic Properties of Free Radicals*, New Series II, Vol. 9b.

(16) Viscosities were measured at 27 °C (the temperature of the TREPR experiment) using an Ubbelohde viscometer.

(17) Carter, K. R.; Miller, R. D.; Hedrick, J. L. *Macromolecules* **1993**, *27*, 2209.

(18) Jeevarajan, A. S.; Fessenden, R. W. *J. Phys. Chem.* **1992**, *96*, 1520.

(19) Musso, H. In *Oxidative Coupling of Phenols*; Taylor, W. I., Battersby, A. R., Eds.; Marcel Dekker: New York, 1967.

(20) (a) Getoff, N. *Radiat. Phys. Chem.* **1989**, *34*, 711. (b) Feitelson, J.; Hayon, E.; Treinin, A. *J. Am. Chem. Soc.* **1973**, *95*, 1025. (c) Feitelson, J.; Hayon, E. *J. Phys. Chem.* **1973**, *77*, 10. (d) Veselov, A. V.; Fessenden, R. W. *J. Phys. Chem.* **1993**, *97*, 3497.

(21) Coggeshall, N. D.; Glessner, A. S., Jr. *J. Am. Chem. Soc.* **1949**, *71*, 3150.

(22) Alfassi, Z. B.; Huie, R. E.; Neta, P. *J. Phys. Chem.* **1986**, *90*, 4156.

(23) Fessenden, R. W.; Schuler, R. H. *J. Chem. Phys.* **1963**, *38*, 773.

(24) (a) Weller, A. *Prog. React. Kinet.* **1961**, *1*, 187. (b) Ireland, J. F.; Wyatt, P. A. H. *Adv. Phys. Org. Chem.* **1976**, *12*, 131.

(25) Forbes, M. D. E.; Dukes, K. E.; Clancy, C. M. R., unpublished results.

MA951381H